Journal of Materials Chemistry B

Accepted Manuscript

ROYAL SOCIETY OF CHEMISTRY

www.rsc.org/materialsB

Journal of Materials Chemistry B

PAPER

On-Demand and Negative-thermo-swelling Tissue Adhesive Based on Highly Branched Ambivalent PEG-catechol Copolymers

Received 00th January 20xx,
Accepted 00th January 20xx

DOI: 10.1039/x0xx00000x

www.rsc.org/MaterialsB

Hong Zhang,[a] Tianyu Zhao,[a] Ben Newland,[b] Patrick Duffy,[a] Aisling Ní Annaidh,[c] Eoin D. O'Cearbhaill,[c,d] and Wenxin Wang*[a]

A series of well-designed highly branched PEG-catechol based thermo-responsive copolymers were synthesized via a one-pot RAFT polymerization. A varying degree of photocrosslinkable (meth)acrylate moieties were incorporated within the 3D structure to allow on-demand photocuring (strong cohesion, unlike conventional PEG adhesives). At the same time, multitudes of free catechol groups inspired from adhesive proteins of marine mussels were also introduced in the hyperbranched structure, giving rise to adherence to skin and cardiac tissue. The resulting ambivalent PEG-catechol based copolymers were systematically studied to investigate the effects of polymer composition on tissue bioadhesive and swelling properties, comparing acrylates to methacrylates and PEG to 2-hydroxyethyl acrylamide (HEAA). It was proved that DOPA played a major role in the adhesion performance as it significantly enhanced the adhesion performances on varied substrates. The highly branched PEG-catechol copolymers demonstrate the great potential in the design of novel surgical glues, sealants or drug delivery vectors.

Introduction

PEG-based adhesives have a long history of use in wound-healing applications to yield a water tight seal or a suture adjuvant that helps hemostasis in the wound.[1] They offer the benefit of good solubility in physiological systems, the ability to avoid immune system recognition (immunological response) and are non-toxic and well tolerated.[2] This family of tissue adhesive typically consists of chemically functionalized linear or star PEGs. Depending on available chemical groups, these modified PEGs can be crosslinked upon mixing through chemical crosslinking or upon photo-curing by irradiation of light to form a hydrogel adhesive.[3] For example, PEG-based hydrogels, commercialized under the brands of FocalSeal®, CoSeal® and DuraSeal™ have been used in cardiovascular, pulmonary, intestinal anastomosis and dural surgical procedures with satisfactory mechanical performance.[1] However, all of the aforementioned PEG-based polymers have some drawbacks that limit their widespread adoption. Firstly, the two-component dual-barrel syringe system for *in situ* chemical crosslinking has a limited working life (polymerize in 5 seconds) and can lead to clogging of the delivery system.[4] Moreover, the PEG-based hydrogels usually have a weak cohesion (internal strength) and the tendency to crystallize resulting in a brittle material, offering poor mechanical performance, due to its low glass transition temperature (T_g<-40 °C).[5] Furthermore, the dramatic swelling property after the application to moist environment is another significant drawback of these PEG hydrogels, especially for those with low crosslinking density limited by the rare reactive end-groups in the molecules. For PEG-based medical adhesives, observed swelling values can rise up to 400 % of the original volume.[6] Swelling of medical adhesives and sealants following deployment can lead to mechanical weakness in the swollen state as well as pressure built up on surrounding tissues such as local nerve compression.[7] Therefore, these PEG-based adhesives are regarded as a valuable add-on to tissue approximation using sutures or staples, but are inappropriate to function as a strong tissue adhesive that can fully replace them.

Inspired by the mussel adhesive proteins, researchers have focused their strategies on the development of biopolymers (e.g., copolypeptides, polystyrene and PEGs) incorporating the catechol functionality.[8] So far, a variety of catechol-modified polymers have been reported, predominantly PEG-catechol hydrogel bioadhesives.[8b,8e] However, to our knowledge, no PEG-catechol polymer with branched structure synthesized by controlled radical polymerization (CRP) has been reported. Herein, we describe the synthesis and characterization of a series of new photocrosslinkable PEG-catechol based highly branched polymer bioadhesives with controllable swelling properties, good adhesion to soft tissue, and considerable mechanical strength, thus addressing some of the limitations of PEG-based adhesives listed above. Firstly, this new robust PEG-based bioadhesive can provide a longer working time with on-demand adhesion upon a short period of UV irradiation (within 1 min) via a free radical mechanism, making it easy to handle, allowing surgeons to make fine adjustments/corrections prior to UV exposure.[9] Secondly, due to the three-dimensional highly branched structure with high amount of photo-activated end-groups, these polymers can reach a high crosslinking density; therefore, strong cohesion strength can be expected in a short time

[a] The Charles Institute of Dermatology, School of Medicine and Medical Science, University College Dublin, Dublin, Ireland.
[b] The Leibniz Institute of Polymer Research Dresden (IPF), Dresden, Germany.
[c] School of Mechanical & Materials Engineering, University College Dublin, Dublin, Ireland.
[d] Conway Institute of Biomolecular and Biomedical Research, University College Dublin, Dublin, Ireland.

† Electronic Supplementary Information (ESI) available: [details of any supplementary information available should be included here]. See DOI: 10.1039/x0xx00000x

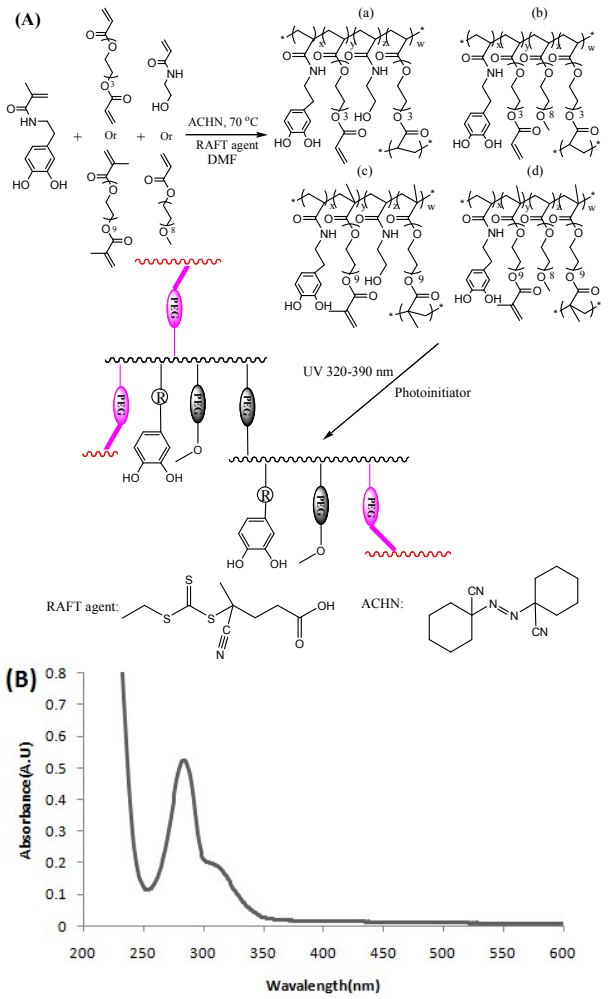

Fig. 1 (A)Representation of the synthesis of (a) P(DMA-HEAA-PEGDA) and (b) P(DMA-PEGMEA-PEGDA) (c) P(DMA-HEAA-PEGDMA) and (d) P(DMA-PEGMEA-PEGDMA) via RAFT polymerization and the cross-linking mechanism through radical photopolymerization by photocleavage after irradiation with 320-390nm UV. (The PEG with acrylate end-groups (pink colors) forms a network after photocuring. DMA = dopamine methacrylamide, PEGMEA = poly(ethylene glycol) methyletheracrylate, HEAA = N-(2-Hydroxyethyl) acrylamide, PEGDA = poly(ethylene glycol) diacrylate, PEGDMA = poly(ethylene glycol) dimethacrylate.) (B)UV-vis spectra of the representative PEG-catechol polymer, with a peak appearing at 280 nm. No detection of a peak after 350nm shows that the PEG-catechol polymer was not oxidized.

following UV light exposure. Thirdly, free catechol groups are introduced to produce PEG−catechol copolymer systems not only possessing high cohesion strength but also the ability to adhere to tissue surfaces.[6b,10] Furthermore, a physiologically useful phase transition temperature(FTT- around 32°C), which immediately relates to the swelling behavior of the hydrogel can be accomplished by altering the hydrophilic and hydrophobic block components in the polymers. Lastly, the covalently formed hydrogels (except for the hydrophobic P(DMA_{40}-$HEAA_{30}$-$PEGDA_{30}$) all exhibit a negative-swelling in physiologic conditions (unlike similar PEG-based systems) in response to the temperature, thus avoiding the possibility of mechanical weakening and tissue-damage associated with exothermic reactions.[11]

In this study, highly branched copolymers composed of an interfacial adhesion segment (dopamine methacrylamide-DMA), a water-soluble segment (poly(ethylene glycol) methyletheracrylate-$PEGMEA_{575}$) or (N-(2-Hydroxyethyl) acrylamide-HEAA) and a cross-linking segment (poly(ethylene glycol) diacrylate-$PEGDA_{258}$) or (poly(ethylene glycol) dimethacrylate-$PEGDMA_{550}$) were synthesized via reversible addition fragmentation chain transfer (RAFT) polymerization **[Fig. 1(A)]**. Polymers with different photo-crosslinking components (acrylate or methacrylate), different hydrophilic components (PEG or HEAA) and their contents were compared. Furthermore, the adhesion properties of DOPA were demonstrateded by comparison of the PEG-DOPA copolymers with previously reported hyperbranched PEG-based copolymer P($PEGDA_{25}$–$PEGMEMA_{50}$) without DOPA[12]. When combined with a photoinitiator (Irgacure 2959), photocrosslinkable bioadhesives could be efficiently achieved by ultraviolet (UV320-390nm) irradiation for one minute. The deactivating nature of RAFT polymerization renders to produce soluble highly branched copolymers with free catechol groups (demonstrated by UV-vis in **Fig. 1(B)**) by copolymerizing with unprotected DMA monomer for biological and biomedical applications. A range of accessible monomers can be used for this controlled living radical polymerization, allowing the combination of DOPA (catechol), HEAA and various formulations of PEG in a highly controlled fashion. This work is the first report of photo-activated highly branched PEG-catechol copolymers synthesized by a one-pot and one-step RAFT polymerization for tissue closure applications. We believe that these new highly branched PEG-catechol copolymers will have huge applications in the design of future synthetic bioadhesives.

Experimental Section

Materials:

Dopamine hydrochloride, sodium borate, sodium bicarbonate, methacrylate anhydride, sodium hydroxide, magnesium sulfate, poly(ethylene glycol) methyletheracrylate(PEGMEA, M_n = 575 $gmol^{-1}$), N-(2-Hydroxyethyl)acrylamide(HEAA), poly(ethylene glycol) diacrylate(PEGDA, M_n = 258 $gmol^{-1}$), poly(ethylene glycol) dimethacrylate (PEGDMA, M_n = 550 $gmol^{-1}$), 1,10-Azobis-cyclohexane-carbonitrile(ACHN), 2,2-dimethoxy-2-phenylacetophenone and pH indicator paper were purchased from Sigma. Tetrahydrofuran, hexane 95%, methylene chloride, ethyl acetate, dimethylformamide, methanol, diethyl ether, hydrochloric acid were purchased from Fisher Scientific. 4-Cyano-4-[(ethylsulfanylthiocarbonyl)sulfanyl] pentanoic acid was obtained as a gift from Dr. Hongyun Tai at Bangor University, UK.

Synthesis of dopamine methacrylamide (DMA):

The reaction media was prepared in 200 ml of distilled water by adding 20 g of sodium borate and 8 g of sodium bicarbonate in order to protect dihydroxy benzene moiety. Both sodium borate and sodium bicarbonate were saturated in water and demonstrated some insolubility. The aqueous solution was degassed by bubbling argon through it for 20 minutes. 10 g of 3,4-dihydroxyphenethylamine hydrochloride was added to this solution. 9.4 ml of methacrylate anhydride solution in 50 ml of tetrahydrofuran (THF) was prepared separately and added dropwise into the aqueous solution containing 3,4-dihydroxyphenethylamine hydrochloride. The pH of the prepared

solution was checked with pH indicator paper. In order to keep the reaction mixture moderately basic (pH 8 or above), 2M NaOH solution was added dropwise. The reaction mixture was stirred for 14 hours at room temperature with argon bubbling through. At this time, a white slurry-like solution had formed which was then washed twice with 100 ml of ethyl acetate. The resulting solid in the solution was centrifuged and the obtained aqueous solution was acidified to pH 2 with 6M of HCl solution. The organic layer of the solution was extracted three times from the acidified aqueous solution with 100 ml of ethyl acetate. The extracted clear brown organic layer in the ethyl acetate was dried over $MgSO_4$. The solution volume was reduced to around 50 ml with a rotary evaporator before the precipitation appeared. The obtained solution was added to 500 ml of hexane with vigorous stirring to precipitate a brownish solid and then the formed suspension was refrigerated to maximize crystal formation size. To purify, the resulting light brown solid was dissolved in 40 ml of ethyl acetate and precipitated in 500 ml of hexane. The final solid powder was dried in a vacuum overnight.

Synthesis of P(DMA-PEGMEA-PEGDA)/P(DMA-PEGMEA-PEGDMA) and P(DMA-HEAA-PEGDA)/ P(DMA-HEAA-PEGDMA):

P(DMA-PEGMEA-PEGDA)copolymers were synthesized by the copolymerization of DMA, PEGMEA (Mn= 575 g mol^{-1}) and multivinyl branching monomer PEGDA (Mn= 258 g mol^{-1}) using reverse addition–fragmentation chain transfer (RAFT) polymerization. Briefly, thecopolymers were prepared in DMF at the concentration of ACHN being 0.012 M in a 100 ml round bottomed flask. The mole ratio of initiator (ACHN), RAFT agent, and all the monomers were always kept at 1:2:100 and among all the monomers DMA always took the mole percentage of 40% with the mole ratio of PEGMEA and PEGDA altered(40:20, 30:30 and 20:40) in order to get copolymers with different branching ratio and amounts of vinyl end groups. The mixtures were stirred until the solution was homogeneous and then was bubbled with argon for 20-25 minutes to remove any oxygen. The reaction was conducted at 70 ˚C in an oil bath while being stirred at 700 rpm until the desired polymer molecular weight, conversion and polydispersity was acquired (monitored by gel permeation chromatography - GPC). To terminate the polymerization, the stopper was removed exposing the reaction to oxygen and cooling the flask rapidly in water. The other four polymers were synthesized using the same methods except that the mole ratio of PEGMEA to PEGDMA kept at 30:30 and 20:40, HEAA to PEGDA/PEGDMA at 30:30. The resulting viscous solution was diluted with 10 ml of MeOH. The diluted solution was added dropwise into 150 ml of diethyl ether with moderate stirring to precipitate the synthesized copolymer. The obtained polymer was dissolved in methylene chloride and precipitated over diethyl ether to purify it. The purified polymer was dried overnight in a vacuum oven. The final product was a light brown color, very sticky and tough.

Characterization of P(DMA-PEGMEA-PEGDA)/P(DMA-PEGMEA-PEGDMA) and P(DMA-HEAA-PEGDA)/ P(DMA-HEAA-PEGDMA) copolymers:

Characterization of the copolymers was carried out by ^{1}H-NMR, GPC and UV-vis. Weight average molecular weight (M_w), number average molecular weight (M_n), polydispersity (PDI, M_w/M_n) and conversion rate were obtained by GPC (Aligent, PL-GPC50) with RI detector. The GPC eluted DMF from columns (2 x Agilent Rapidgel, 5µm, Mixed C 300mm x 7.5 mm) and calibration was carried out using poly (methyl methacrylate) standards. Analysis and calibration was carried out at 60 ˚C at a flow rate of 1mL/min. ^{1}H NMR was carried out on a 400 MHz Bruker NMR with Delta NMR processing software. The oxidation state of catechol-containing polymers used in this study were confirmed by UV-vis spectroscopy measuring absorbance from 200-600 nm with ultrapure water as a control.

Preparation and characterization of photocured adhesive samples by lap-shear tests:

For shear-lap tests on borosilicate glass, each copolymer (50 mg) was dissolved in photoinitiator Irgacure 2959 solution (2,2-dimethoxy-2-phenylacetophenone,200 µL,1% (w/v) in methylene chloride). For shear-lap tests on porcine skin, P(DMA_{40}-$PEGMEA_{20}$-$PEGDMA_{40}$) copolymer (100 mg) was dissolved in photoinitiator aqueous solution (500 µL,1% (w/v). The adherends (borosilicate glass or porcine skin sample) applied with the polymer adhesive (an area of 2.0 × 2.5 cm), were overlapped with a borosilicate glass adherend and allowed to cure for 60 s with a spot-curing UV light source (OmniCure S1000, LumenDynamicsGroup Inc.) equipped with a filter in the range of 320 to 390 nm when using a light intensity of 0.40 W/cm^2.The lap-shear tests were performed using a Hounsfield universal testing system right after 60 s cure at room temperature. Each measurement was repeated 5 times, averaged, and error bars of 80% confidence intervals are shown.

Preparation and characterization of photocured adhesive samples by uniaxial tensile tests on bovine heart tissue:

Bovine heart tissue samples were kept moist at all times by keeping in PBS buffer solution before use. The samples were cut to 30 mm wide, 40 mm long, and approximately 10 mm thick. An incision, 10mm wide was made in the center of the specimen, and cut to a depth of approximately 50% of the specimen thickness. The interior of the incision was dabbed with tissue to remove excess water on the surface of the sample before the test. P(DMA_{40}-$PEGMEA_{20}$-$PEGDMA_{40}$) was dissolved in distilled water at a concentration of 15% w/v. 100µL of the polymer adhesive was pipetted into the incision and the incision closed by hand. The samples were then allowed to cure 60 s with a spot-curing UV light source using a light intensity of 0.40 W/cm^2. To secure the lamb heart sample in the tensile testing machine, teflon string and small fish hooks were used. Teflon string was used as it is a very strong material and would not deform under the tensile load. Fish hooks were sourced from a local fish tackle shop. Three hooks were hooked evenly apart at either end of the sample and on opposite sides of the incision. Nylon

Table 1 Copolymerization of DMA, $PEGMEA_{575}$/HEAA and $PEGDA_{258}$/$PEGDMA_{550}$ via RAFT polymerization, using 1,10-Azobis-cyclohexane-carbonitrile (ACHN) as initiator, 4-cyano-4-[(ethylsulfanylthiocarbonyl)sulfanyl] pentanoic acid as RAFT agent and DMF as solvent with ACHN concentration of 0.012M and the mole ratio of initiator (ACHN), RAFT agent, and all the monomers kept at 1:2:100 at 70˚C.

Entry	Polymer	RT[a]	MC[b]	M_w(PDI)[c]	FTT[d]	DOPA[e]	PEG[e]	Vinyl[e]	BR[e]	AS(kPa)[f]
1-1	P(DMA_{40}-$PEGMEA_{40}$-$PEGDA_{20}$)	17h	95.6%	18.8k (1.6)	32^{o}C	42.8%	57.2%	4.6%	6.5%	16.1(Co)

1-2	P(DMA_{40}-$PEGMEA_{30}$-$PEGDA_{30}$)	13h	90.6%	15.0k (1.5)	22°C	36.5%	63.5%	10.9%	13.4%	41.6(Co)
1-3	P(DMA_{40}-$PEGMEA_{20}$-$PEGDA_{40}$)	11h	80.8%	14.2k (1.6)	15°C	36.0%	64.0%	17.5%	21.6%	149.7(Ad)
2-1	P(DMA_{40}-$PEGMEA_{30}$-$PEGDMA_{30}$)	6h	74.4%	11.2k (1.5)	23°C	31.4%	68.6%	13.7%	26.1%	105.2(Co)
2-2	P(DMA_{40}-$PEGMEA_{20}$-$PEGDMA_{40}$)	5h	61.9%	13.6k (1.4)	30°C	25.0%	75.0%	10.6%	34.3%	208.9(Ad)
3	P(DMA_{40}-$HEAA_{30}$-$PEGDA_{30}$)	15h	77.2%	14.8k (1.6)	NA	28.0%	44.5%	13.2%	31.3%	81.6(Co)
4	P(DMA_{40}-$HEAA_{30}$-$PEGDMA_{30}$)	9h	55.9%	11.1k (1.4)	10°C	31.5%	47.1%	22.3%	24.8%	316.3(Ad)

[a] Reaction time; [b] Monomer conversion estimated from copolymer and monomer peaks in GPC traces; [c] M_w–weight average molecular weight, PDI-polydispersity index (M_w/M_n); [d] FTT-the phase transition temperature at the polymer concentration of ~10% w/v which was monitored by raising the temperature from 5 to 35˚C and measuring the temperature at the onset of cloudiness; [e] Final DOPA composition, PEG composition, vinyl groups content and branching ratio within the polymer structure calculated by ^{1}H NMR; [f] Adhesion strength was tested by shear-lap tests on borosilicate glass (n = 5) and the average value was presented here along with the failure type (Co-cohesive or Ad-adhesive failure) by dividing recorded maximum load (force) by overlapped borosilicate glass surface area.

holders allowed the Teflon string to be secured to both members of the tensile testing machine. The sample was handled with care to ensure that the glued incision was not ruptured. As the test was carried out, the incision on the lamb heart sample was closely observed. The type of failure of the adhesive and the force at which it failed was noted. This allowed the point on the stress-strain curve where the adhesive failed to be identified.

Rheological properties of Hydrogel

Real-time photocrosslinking rheological studies were performed on P(DMA_{40}-$PEGMEA_{20}$-$PEGDMA_{40}$) with a UV light source (UV320-390 nm, Omnicure1000, light intensity of 0.40 W/cm^2). The bottom plate was made of PMMA through which the samples were exposed to UV light. The oscillatory measurements were performed at 25°C, respectively, for 200 s, with a frequency of 10 Hz, a strain of 0.5%, and a gap of 0.3 mm. The strain was within the linear viscoelastic region. The samples were exposed to UV light for 2 min after the first minute of data collection.

Swelling of Hydrogels:

Hydrogels were formed using ice cold water by 2 mins UV curing at a light intensity of 0.40 W/cm^2 respectively on both sides. To observe thermo-reversible swelling properties of the hydrogels, the changes in swelling between two fixed temperatures (20 °C or 37 °C) were obtained by alternatively placing the samples in two water baths with different temperatures in every 4 hours. After every 4 hours, samples were removed from PBS, blotted to remove excess surface water, and weighed. Swelling Ratio (SR) was calculated by $SR= (m_f-m_i)/m_i$ (1), where mf and mi represent the initial and final mass of the hydrogels, respectively. Five replicates were performed and the average value was reported.

Cytotoxicity Assays:

To quantitatively assess *in vitro* cytotoxicity of PEG-DOPA copolymers, viability assay was performed. First, the solution of different copolymers (1-1, 1-2, 1-3, 2-1 and 2-2) in Dulbecco's modified Eagle's medium (DMEM), containing 10% (v/v) fetal bovine serum (FBS) and 1% (v/v) streptomycin, were prepared in four different concentrations: 10, 5, 1, 0.5 and 0.1 mg/mL. Next, 200µL of a solution of 3T3 fibroblast cells in DMEM (5×10^4 cells/mL) was added and incubated for 24 hours at 37°C, 5% CO_2 and 95% relative humidity in a 96-well cell culture plate. The medium of each well was then replaced by polymer-containing DMEM solutions with various concentrations and incubated for another 24 hours followed by the standard alamarblue® assay. Viability of cells in the DMEM containing polymers were normalized to that of cells cultured in blank medium (DMEM without polymers) as control.

In order to assess the cytotoxicity of the extracts of PEG-DOPA gel, the prepared gel samples (100 mg) were first soaked in PBS (pH 7.4) for 24 h and then they were sterilized with UV light for 30 mins and placed in wells of 24-well culture plate which already contained 1 mL DMEM. After 24 h, three different extract solutions were prepared: 1×, 10× and 100× (1× was the solution of leached products without dilution; 10× and 100× means 10 times and 100 times dilution with medium, respectively) and were used for cell culture after removing the gels. 3T3 fibroblast cells were seeded in wells of 96-well plates with a density of 10^4 cells per well. The viabilities of cells were evaluated using the standard alamarblue® assay after another 24 h incubation by normalizing metabolic activity to cells which were cultured in the blank medium.

Results and Discussions

One of the most common and facile synthesis methods is to polymerize vinyl monomers bearing unprotected catechols by free radical polymerization. A random copolymer P(DMA-co-MEA) containing 11.3 mol% DMA synthesized by free radical copolymerization of dopamine methacrylamide with methoxyethyl acrylate was firstly reported by Messersmith et al. P(DMA-co-MEA) was demonstrated to have reversible attachment to a variety of surfaces in any environment.[13] Inspired by the pioneering work, the (un)protected version catechol-functionalized monomer was copolymerized with more common monomers such as methyl methacrylate,[8c] styrene,[8d] acrylamide[8a] and more predominantly, PEG-(meth)acrylates,[8b,14] employing conventional free radical polymerization (FRP) methods in several scientific groups. However, the controlled synthesis of catechol-bearing polymers by routine CRP techniques, is limited by the presence of the unprotected catechols, which are known to be radical scavengers and prone to oxidize, and thus might inhibit or impede the radical polymerization.[15] In this study, a range of highly branched PEG-catechol based copolymers with different amounts of photo-reactive (meth)acrylate groups and varying branching ratios were synthesized by altering the feed ratio as shown in **Table 1**. The free pendent catechol functionality was successfully introduced into these highly branched PEG copolymers by copolymerizing with unprotected DMA monomer and the DOPA (catechol) ratio was

designed to remain constant by holding the DMA component feeding ratio at 40 mol% throughout all reactions. DMA was prepared from the reaction of 3,4-dihydroxyphenethylamine hydrochloride and methacrylate anhydride in an aqueous solution of sodium borate and sodium bicarbonate with a liaccording to a previously reported technique.[13,16] The synthesized DMA monomer was a solid pale-gray powder prepared in a yield of 64%. Proton nuclear magnetic resonance (^{1}H NMR) spectral analysis on samples of the synthesized DMA **(Figure S1)** and all copolymers **(FigureS2-S5)** were performed to confirm that the resulting materials had the desired chemical structure. 40mol% feeding ratio of DMA is chosen here as the final copolymers comprise around 30±10mol% DOPA content **(Table 1)** and it has been reported that around 30% DOPA maximized adhesion without too much cross-linking being a detriment to function.[8d] During the reaction the polymer chain growth was monitored using gel permeation chromatography (GPC) analysis (**Figure S6**). Reaction time for comparable molecular weights was shorter when a higher ratio of crosslinking PEGDA or PEGDMA was involved while the monomer conversion rate was lower (entry 1-1, 1-2, 1-3, Table 1). Even if a high concentration of PEGDA was chosen (40 mol%), a copolymer with a final conversion of 80.8 % after 11 h of polymerization was accomplished (entry 1-3, Table 1), incorporating a high degree of vinyl functionality (17.5 mol%) and branching (21.6 mol%) within its structure (entry 1-3,Table 1). With PEGDMA as the crosslinking segment, the polymerization rate is much faster (see entry 2-1, 2-2, Table 1). HEAA was also used as hydrophilic segment to replace PEGMEA with lower PEG content in the copolymer. The polymer composition is outlined in Table 1 showing the vinyl group content and branching degree of the copolymers. Except for P(DMA_{40}-$HEAA_{30}$-$PEGDA_{30}$), all copolymers show good solubility in water below the phase transition temperature (FTT) (Table 1). From FTT data, we can conclude more hydrophilic co-monomer generally increases the FTT of the copolymer (compare entry 1-1, 1-2 and 1-3, Table 1).

The curing of these DOPA-containing compounds was typically accomplished by oxidation of DOPA residues to form DOPA-quinone, which participated in intra- and/or intermolecular cross-linking reactions to form a gel network. However, it has been reported that the oxidized forms of DOPA are believed to be less adhesive than unoxidized DOPA. DOPA-containing proteins and polymers exhibit better adhesion to both metallic and mucosal surfaces when DOPA residues are not oxidized.[17] In this study, both DOPA and (meth)acrylate terminal functionalities coexist in the highly branched structure. Thus, we preserved the unoxidized adhesive form of DOPA in hydrogel formation by utilizing the methacrylate via photocrosslinking. The effect of PEG content, acrylate or methacrylate content and highly branched structure on bonding performance of the pure copolymer was further evaluated through lap-shear adhesion tests after photo-crosslinking with the control of hyperbranched PEG-based copolymer P($PEGDA_{25}$–$PEGMEMA_{50}$) bearing 12.8 mol% vinyl content and 20.0 mol% branching ratio (FigureS7). Borosilicate glass was used as the bonding surfaces due to the well defined surface area and UV light transparency. Comparing the copolymer with 20% and 30% molar ratio of PEGDA, P(DMA_{40}-$PEGMEA_{20}$-$PEGDA_{40}$) possessed the highest lap-shear strength (149.7 kPa) as a lower degree of vinyl end groups resulted in cohesive failure of the material owing to its limited cross-linking(entry 1-1, 1-2, 1-3, Table 1). P(DMA_{40}-$PEGMEA_{20}$-$PEGDMA_{40}$) also showed an improved adhesion strength compared to P(DMA_{40}-$PEGMEA_{30}$-$PEGDMA_{30}$), probably because of a stronger cohesive strength arising from a higher branching ratio as well as a relative lower DOPA ratio which accelerated the photocuring rate (entry 2-1, 2-2, Table 1). When using the same feeding ratio of crosslinking component, the copolymer with PEGDMA tended to obtain an increased lap-shear strength, which may be due to a faster/more complete UV crosslinking, as typically PEGDMA is more reactive compared to PEGDA. Comparing entry 1-2 with 3 and 2-1 with 4 (Table 1), it can be seen that the copolymer with less PEG composition ratio had a higher lap-shear strength. It is possible that an increase in PEG composition limits the adhesion capabilities given that PEG may prevent interactions with other molecules.[8b,18] We can also conclude that DOPA plays a major role for overall tissue and surface adhesion when comparing entry 1-3 with the

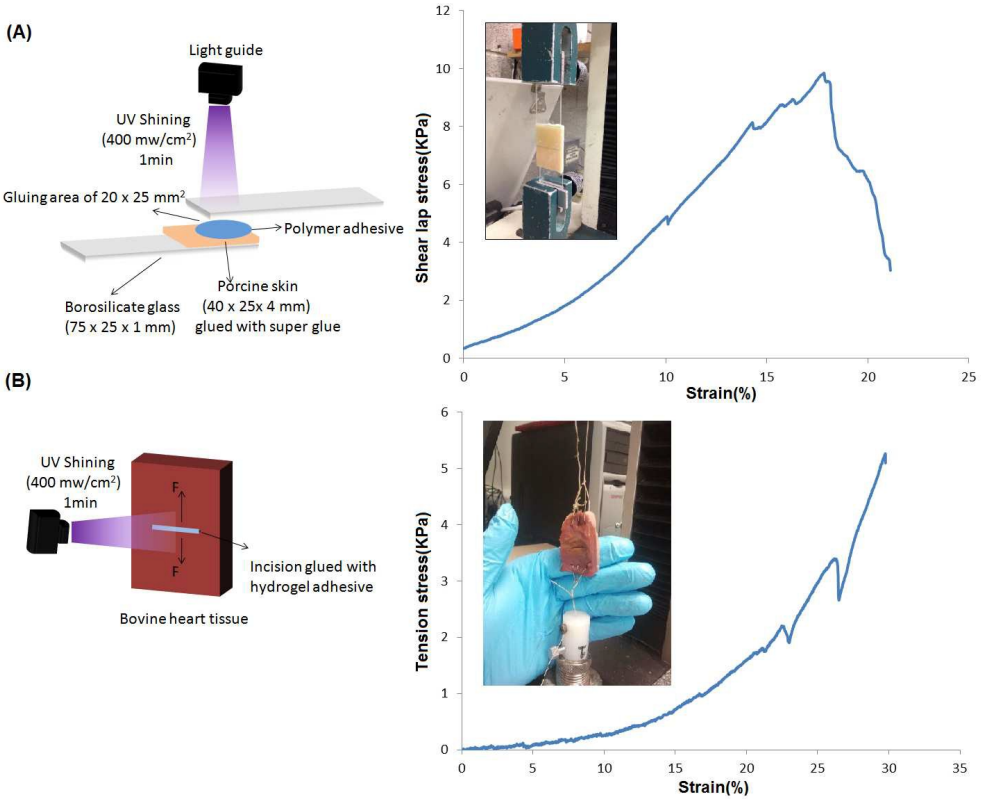

Fig.2 (A) Schematic of sample preparation prior to shear-lap test and stress-strain curve of porcine skin sample glued with P(DMA_{40}-$PEGMEA_{20}$-$PEGDMA_{40}$) under lap-shear tensile test (B) Schematic of sample preparation prior to tensile testing and typical stress-strain curve of an idealized bovine heart tissue wound model with an incision (10 mm long and 5 mm deep) glued with P(DMA_{40}-$PEGMEA_{20}$-$PEGDMA_{40}$).

control P($PEGDA_{25}$–$PEGMEMA_{50}$) polymer having similar vinyl content and branching ratio but lacking DOPA **(FigureS7)**. The mechanical properties of the photocrosslinked P(DMA_{40}-$PEGMEA_{20}$-$PEGDMA_{40}$) hydrogel was also studied by *in situ* photocrosslinking rheology experiments in the presence of photoinitiator Irgacure 2959. The samples were exposed to UV light for 2mins after the first minute of data collection. The results showed that the crossover of G' and G'' occurred within 25 seconds of UV exposure, suggesting the start of the polymerization and leading to photocrosslinked gels with moduli 3 orders of magnitude greater than uncrosslinked polymers and then a plateau value in the hydrogel storage modulus was reached **(FigureS8)**. These results suggest that P(DMA_{40}-$PEGMEA_{20}$-$PEGDMA_{40}$) polymer solutions underwent fast photopolymerization and reached almost complete gelation within 60 seconds.

P(DMA_{40}-$PEGMEA_{20}$-$PEGDMA_{40}$) hydrogel was also evaluated as an adhesive on porcine skin and heart tissue to obtain some preliminary data by including the control of P($PEGDA_{25}$–$PEGMEMA_{50}$) polymer lacking DOPA. After 1 min UV curing, approximately 10 kPa adhesion strength can be achieved under shear stress on porcine skin samples and 5 kPa adhesion under tensile stress in a bovine heart tissue wound model **(Fig.2)**. In comparison, P($PEGDA_{25}$–$PEGMEMA_{50}$) showed a very low adhesion strength on soft tissue and failed to produce any stable results. Despite a retarding inhibitory effect of DOPA on photopolymerization due to the phenolic nature of the catechol side chain of DOPA,[19] P(DMA_{40}-$PEGMEA_{20}$-$PEGDMA_{40}$) hydrogels do not require oxidizing reagents to gel and possess mechanical stress sufficient for use in many biomedical application with an on-demand adhesion mechanism.

To investigate the cytotoxicity of PEG-DOPA copolymers, cell metabolic activity was measured, as shown in **Fig. 3(A)**. We observed moderate toxicity with a cell metabolic activity between 63±4 and 56±3 % of that in the blank medium when copolymers with acrylate end-groups (1-2 and 1-3) at the concentration of 1 mg/mL were utilized. In diluted solutions of 0.5 and 0.1 mg/mL, the cell metabolic activity was between 75±3 and 90±5 %. However,

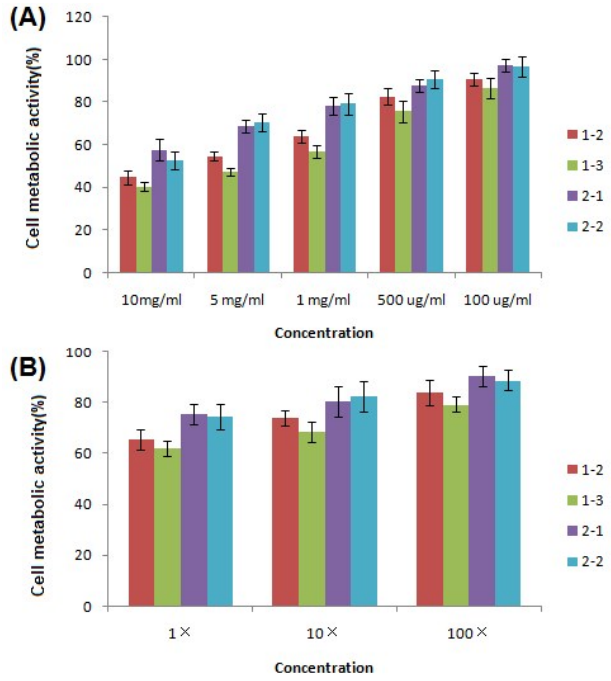

Fig.3 Alamarblue® assay based cytotoxicity study with 3T3 fibroblast cells: A) PEG-DOPA copolymers B) Leachable products (sol content) of PEG-DOPA gels. All data were normalized to cell metabolic activity in blank medium.

PEG-DOPA copolymers with methacrylate groups (2-1 and 2-2) only showed minimally reduced metabolic performance (around 70±3 %) even at a higher concentration (5 mg/mL), demonstrating better cell metabolic activity than copolymers with acrylate groups. When the concentration of PEG-DOPA copolymers with methacrylate groups (2-1 and 2-2) come up to 10 mg/mL, moderate toxicity with a cell metabolic activity 55±3% of that in the blank medium was measured. We assume the toxicity is mainly due to the reactivity of the methacrylate and especially acrylate double bond towards Michael addition reactions with amino- or thiol-groups of proteins.[20] It has been reported that autoxidation of these catechol species generates a considerable amount of reactive oxygen species (ROS) and also quinone, which may increase cytotoxicity.[21] Hydrogen peroxide (H_2O_2) is a major component of ROS that has been detected in cell culture media containing DOPA.[22] However, 2-1 (P(DMA_{40}-$PEGMEA_{30}$-$PEGDMA_{30}$) copolymer with a higher DOPA ratio (31.4%) did not exhibit significant toxicity difference with 2-2 (P(DMA_{40}-$PEGMEA_{20}$-$PEGDMA_{40}$) copolymer having a lower DOPA ratio (25.0%), probably due to the fact that the catechol groups synthesized from RAFT polymerization are quite stable (proved by UV-vis in Fig. 1B). The metabolic activity of cells exposed to the leachable content (sol content) of crosslinked PEG-DOPA gels (10 wt%) with acrylate groups (1-2 and 1-3) at 1× concentration was between 55±4 and 52±3 % of the control, inferring moderate cytotoxicity. The leachable product (1×) of PEG-DOPA gels with methacrylate groups (2-1 and 2-2) resulted in a relative cell metabolic activity of at least 65±3%, suggesting that the leachable products did not induce significant cytotoxicity **(Fig. 3B)**. Furthermore, compared to the cytotoxicity of PEG-DOPA copolymers, leachable products (1×) from PEG-DOPA gels showed notably higher cell metabolic activity, probably due to the consumption of (meth)acrylate groups during the photocrosslinking process.

Swelling due to water absorption is a general feature of chemically hydrophilic cross-linked polymer networks. Usually the swelling of hydrogels significantly depends on the hydrophilicity, polymer architecture, the degree of crosslinking density and polymer volume fraction.[23] With reference to thermo-responsive polymers, covalently linked networks exhibit a change in their degree of swelling in response to temperature, **Fig. 4(A)**, whereas physical gels show a sol-gel transition.[24] To circumvent the shortcomings caused by significant swelling upon immersion into excess water, which happens in most *in-situ* forming hydrogel sealants,[6] we sought to utilize the thermally induced transition from hydrophilic to hydrophobic in aqueous systems by altering the hydrophilic and hydrophobic block components in their network structure to induce gel contraction as a way to modulate the swelling behavior. To confirm the thermo-responsive properties, the swelling ratio of the hydrogels (10 wt%) was measured during temperature fluctuations. Here, the hydrogel samples were alternatively placed in the thermostat baths at 20 or 37 ^{o}C, and their swelling changes were measured **(Fig. 4B)** every 4 hours. Figure 4(B) shows the effect of temperature on the swelling ratio. It was observed that at 20^{o}C, swelling values of copolymers with FTT ≥ 22^{o}C range from 8.2 % to 25.4 % increasing with the hydrophilicity of the co-monomer ($PEGDMA_{550}$ is hydrophilic while $PEGDA_{258}$ is hydrophobic) and decreasing with the crosslinking density of the copolymer. Our previous research has demonstrated that 10% hyperbranched PEG copolymer with around 20% hyperbranching can reach a maximum of 80% swelling ratio in 48 h.[12] We attribute the decreased swelling behavior to the hydrophobic nature of the fully protonated form of DOPA at pH values below 10.5.[25] On the contrary, gel 1-3 and 4 with FTT < 20^{o}C contracted 21.0-50.6% presumably because of the enhanced hydrophobic interaction at temperatures higher than FTT leading to a collapse of chains into hydrophobic domains (Fig. 4A).[24b,26] It was interesting to note that, all hydrogels exhibited a negative thermo-responsive swelling behavior. Exposure of the hydrogels to a higher temperature (37^{o}C) led to shrinking in volume. For Gel 1-3 and Gel 4, they contracted more at 37^{o}C than at 20^{o}C. Comparing HEAA containing copolymer with PEGMEA containing copolymer, we can see incorporation of more PEG reduced de-swelling and shrinkage of the gel confirming other work indicating that increasing PEG content decreased the thermo-responsiveness and slows the phase transition of such copolymers.[27] When the hydrogels were exposed to 20 ^{o}C again, they recovered their initial swelling ratio. Swelling of the hydrogels was reversibly changed between the two temperatures. The interesting swelling properties of the copolymers show they may find some potential applications in drug delivery as the decrease in the volume of the gel will result in release of entrapped drug.

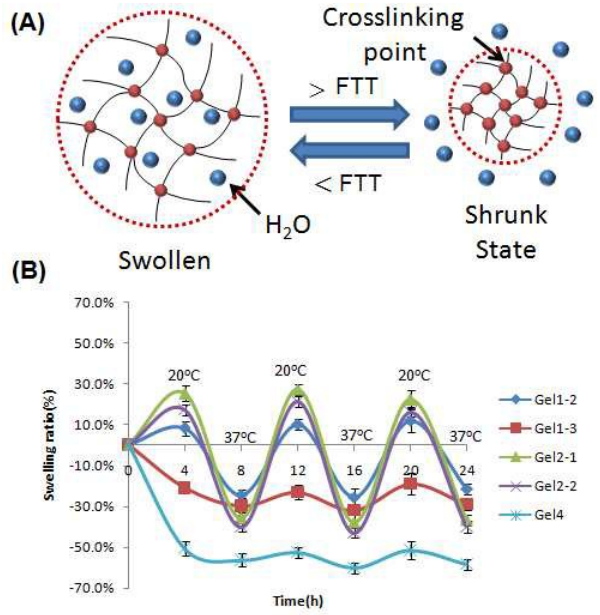

Fig.4 (A) Schematic representation of a gel in its shrunken and swollen states. The red and blue points correspond to crosslinking points and water, respectively. (B) Thermo-swelling reversibility of DOPA-PEG gels as a function of gel formation temperature. Gels were studied in the temperature-based experiments at 20°C and 37°C alternatively.

Conclusions

In conclusion, we describe the design and synthesis of hydrogel adhesives, which combine a mussel inspired adhesion component DOPA, with a biocompatible PEG segment in a highly branched structure. The resulting polymer forms gels in a short time after UV curing, and these gels possess strong cohesive strength. The lap-shear strength of the adhesives could be increased by substituting HEAA for PEGMEA (i.e. reducing the PEG content) and it was found that those containing the crosslinking segment PEGDMA were stronger than those with PEGDA. The tissue adhesive potential was demonstrated through lap-shear adhesion measurements on both borosilicate glass and porcine skin, and also through tensile test measurements on a bovine heart tissue wound model, producing bond strengths greater than PEG-based adhesives. This novel class of thermo-sensitive copolymers with low cytotoxicity represents a facile and versatile synthetic route to strong mussel-inspired polymer hydrogels with an accurately controlled swelling to fit in different clinical application through variation of polymer composition and structure.

Acknowledgements

Health Research Board (HRB) of Ireland and Science Foundation Ireland (SFI), SFI Principal Investigator programme, DEBRA Ireland, University College Dublin, Strategic and Major Initiative 2014 are gratefully acknowledged for funding.

Notes and references

1 (a) M. S. Allen, D. E. Wood, R. W. Hawkinson, D. H. Harpole, R. J. McKenna, G. L. Walsh, E. Vallieres, D. L. Miller, F. C. Nichols, W. R. Smythe, R. D. Davis, M. T. M. S. S. S. Grp, *Annals of Thoracic Surgery* **2004**, *77*, 1792-1801; (b) G. R. Cosgrove, J. B. Delashaw, J. A. Grotenhuis, J. M. Tew, H. van Loveren, R. F. Spetzler, T. Payner, G. Rosseau, M. E. Shaffrey, L. N. Hopkins, R. Byrne, A. Norbash, *Journal of Neurosurgery* **2007**, *106*, 52-58; (c) R. Fasol, T. Wild, S. El Dsoki, *Annals of Thoracic Surgery* **2004**, *77*, 1070-1072; (d) A. M. Gillinov, B. W. Lytle, *Journal of Cardiac Surgery* **2001**, *16*, 255-257; (e) C. Pace Napoleone, A. Valori, G. Crupi, S. Ocello, F. Santoro, P. Vouhe, N. Weerasena, G. Gargiulo, *Interactive Cardiovascular and Thoracic Surgery* **2009**, *9*, 978-982.

2 (a) A. L. Klibanov, K. Maruyama, V. P. Torchilin, L. Huang, *Febs Letters* **1990**, *268*, 235-237; (b) K. Knop, R. Hoogenboom, D. Fischer, U. S. Schubert, *Angewandte Chemie-International Edition* **2010**, *49*, 6288-6308.

3 M. Mehdizadeh, J. Yang, *Macromolecular Bioscience* **2013**, *13*, 271-288.

4 (a)Hill, A.; Estridge, T. D.; Maroney, M.; Monnet, E.; Egbert, B.; Cruise, G.; Coker, G. T. *Journal of Biomedical Materials Research* **2001**, *58*, 308; (b)DeAnda, A.; Elefteriades, J. A.; Hasaniya, N. W.; Lattouf, O. M.; Lazzara, R. R. *Journal of Cardiac Surgery* **2009**, *24*, 325.

5 C. Golander, J. Herron, K. Lim, P. Claesson, P. Stenius, J. Andrade, J. Harris, Plenum Press, New York, **1992**.

6 (a) H. K. Cho, S. T. Noh, *Journal of Industrial and Engineering Chemistry* **2000**, *6*, 19-24; (b) C. E. Brubaker, P. B. Messersmith, *Biomacromolecules* **2011**, *12*, 4326-4334.

7 (a) G. Lee, C. K. Lee, M. Bynevelt, *Spine* **2010**, *35*, E1522-E1524; (b) D. Thavarajah, P. De Lacy, R. Hussain, R. M. Redfern, *Spine* **2010**, *35*, E25-E26.

8 (a) E. M. White, J. E. Seppala, P. M. Rushworth, B. W. Ritchie, S. Sharma, J. Locklin, *Macromolecules* **2013**, *46*, 8882-8887; (b) C. R. Matos-Perez, J. J. Wilker, *Macromolecules* **2012**, *45*, 6634-6639; (c) J. H. Cho, K. Shanmuganathan, C. J. Ellison, *Acs Applied Materials & Interfaces* **2013**, *5*, 3794-3802; (d) C. R. Matos-Perez, J. D. White, J. J. Wilker, *Journal of the American Chemical Society* **2012**, *134*, 9498-9505; (e) Hong, S.; Lee, H.; Lee, H. Beilstein, *Journal of Nanotechnology* **2014**, *5*, 887.

9 (a) K. T. Nguyen, J. L. West, *Biomaterials* **2002**, *23*, 4307-4314; (b) N. Lang, M. J. Pereira, Y. H. Lee, I. Friehs, N. V. Vasilyev, E. N. Feins, K. Ablasser, E. D. O'Cearbhaill, C. J. Xu, A. Fabozzo, R. Padera, S. Wasserman, F. Freudenthal, L. S. Ferreira, R. Langer, J. M. Karp, P. J. Nido, Science Translational Medicine **2014**, *6*(218).C

10 (a) M. Mehdizadeh, H. Weng, D. Gyawali, L. Tang, J. Yang, *Biomaterials* **2012**, *33*, 7972-7983; (b) H. Zhang, L. P. Bre, T. Zhao, Y. Zheng, B. Newland, W. Wang, *Biomaterials* **2014**, *35*, 711-719; (c) H. Zhang, L. Bre, T. Zhao, B. Newland, M. Da Costa, W. Wang, *Journal of Materials Chemistry B* **2014**, *2*, 4067-4071.

11 W. D. Spotnitz, S. Burks, *Transfusion* **2008**, *48*, 1502-1516.

12. R. Kennedy, W. Ul Hassan, A. Tochwin, T. Zhao, Y. Dong, Q. Wang, H. Tai, W. Wang, *Polymer Chemistry* **2014**, *5*, 1838-1842.

13 P. Glass, H. Chung, N. R. Washburn, M. Sitti, *Langmuir* **2009**, *25*, 6607-6612.

14 H. Han, J. Wu, C. W. Avery, M. Mizutani, X. Jiang, M. Kamigaito, Z. Chen, C. Xi, K. Kuroda, *Langmuir* **2011**, *27*, 4010-4019.

15 E. Faure, C. Falentin-Daudre, C. Jerome, J. Lyskawa, D. Fournier, P. Woisel, C. Detrembleur, *Progress in Polymer Science* **2013**, *38*, 236-270.

16 H. Lee, B. P. Lee, P. B. Messersmith, *Nature* **2007**, *448*, 338-U334.

17 (a) M. E. Yu, J. Y. Hwang, T. J. Deming, *Journal of the American Chemical Society* **1999**, *121*, 5825-5826; (b) M. E. Yu, T. J. Deming, *Macromolecules* **1998**, *31*, 4739-4745.

18 S. Yuan, D. Wan, B. Liang, S. O. Pehkonen, Y. P. Ting, K. G. Neoh, E. T. Kang, *Langmuir* **2011**, *27*, 2761-2774.

19 (a) B. P. Lee, C. Y. Chao, F. N. Nunalee, E. Motan, K. R. Shull, P. B. Messersmith, *Macromolecules* **2006**, *39*, 1740-1748; (b) S. Fujisawa, M. Ishihara, Y. Kadoma, *Sar and Qsar in Environmental Research* **2002**, *13*, 617-627.
20 (a) B. Husar, C. Heller, M. Schwentenwein, A. Mautner, F. Varga, T. Koch, J. Stampfl, R. Liska, *Journal of Polymer Science Part a-Polymer Chemistry* **2011**, *49*, 4927-4934; (b) C. Dworak, T. Koch, F. Varga, R. Liska, *Journal of Polymer Science Part a-Polymer Chemistry* **2010**, *48*, 2916-2924; (c) S. Hong, K. Yang, B. Kang, C. Lee, I. T. Song, E. Byun, K. I. Park, S.-W. Cho, H. Lee, *Advanced Functional Materials* **2013**, *23*, 1774-1780.
21 (a) L. K. T. Lam, P. K. Garg, S. M. Swanson, J. M. Pezzuto, *Journal of Pharmaceutical Sciences* **1988**, *77*, 393-395; (b) S. Mansoor, N. Gupta, G. Luczy-Bachman, G. A. Limb, B. D. Kuppermann, M. C. Kenney, *Toxicology* **2010**, *271*, 107-114; (c) J. Hirrlinger, J. B. Schulz, R. Dringen, *Journal of Neurochemistry* **2002**, *82*, 458-467.
22 E. Eruslanov, S. Kusmartsev, in *Advanced Protocols in Oxidative Stress Ii, Vol. 594* (Ed.: D. Armstrong), **2010**, pp. 57-72.
23 Y. Dong, P. Gunning, H. Cao, A. Mathew, B. Newland, A. O. Saeed, J. P. Magnusson, C. Alexander, H. Tai, A. Pandit, W. Wang, *Polymer Chemistry* **2010**, *1*, 827-830.
24 (a) Y. Dong, W. Hassan, Y. Zheng, A. O. Saeed, H. Cao, H. Tai, A. Pandit, W. Wang, *Journal of Materials Science-Materials in Medicine* **2012**, *23*, 25-35; (b) S. J. Im, Y. M. Choi, E. Subrarnanyarn, K. M. Huh, K. Park, *Macromolecular Research* **2007**, *15*, 363-369; (c) D. G. Barrett, G. G. Bushnell, P. B. Messersmith, *Advanced Healthcare Materials* **2013**, *2*, 745-755; (d)He, X.; Fan, J.; Zhang, F.; Li, R.; Pollack, K. A.; Raymond, J. E.; Zou, J.; Wooley, K. L, *Journal of Materials Chemistry B* **2014**, *2*, 8123.
25 M. Guvendiren, P. B. Messersmith, K. R. Shull, *Biomacromolecules* **2008**, *9*, 122-128.
26 M. A. Ward, T. K. Georgiou, *Polymers* **2011**, *3*, 1215-1242.
27 (a) J. F. Pollock, K. E. Healy, *Acta Biomaterialia* **2010**, *6*, 1307-1318; (b) J. Virtanen, H. Tenhu, *Macromolecules* **2000**, *33*, 5970-5975.

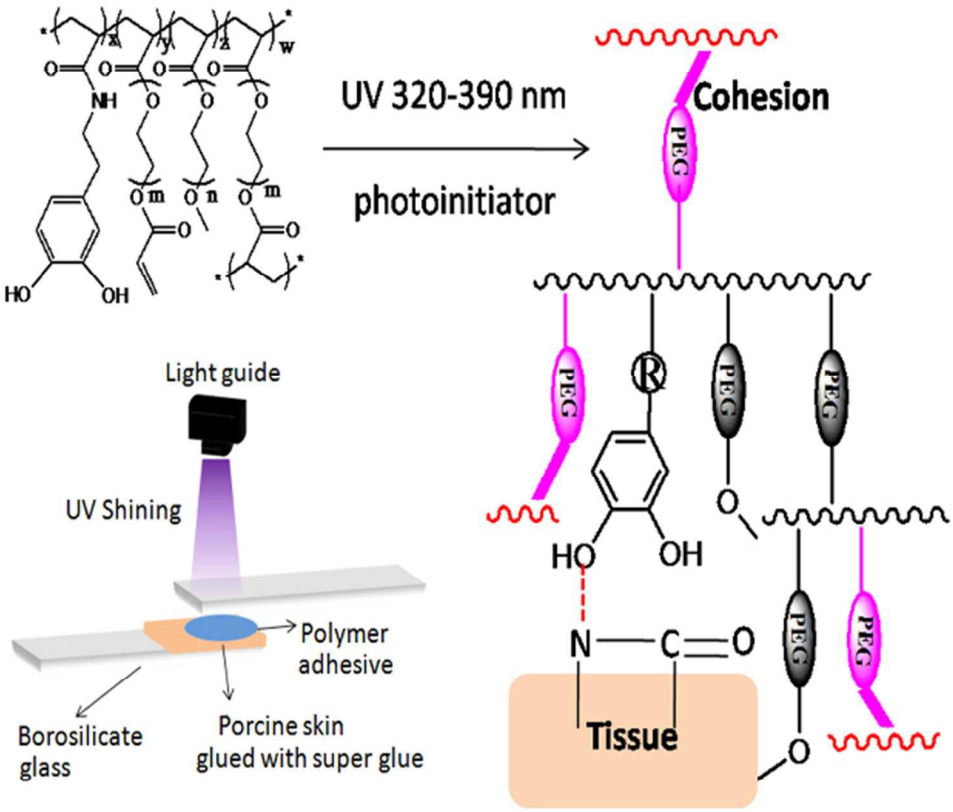

55x50mm (300 x 300 DPI)